

**Inversion of Stereoselectivity by Hydrophobic Interligand Interactions.
Preparation, Structure, and Stereoselectivity of
{*N,N'*-Ethylenebis(1,1,1-trifluoro-4-
amino-2-pentanonato)}(L-amino
acidato)cobalt(III)**

Yuki FUJII,* Homare SHINOHARA, Masahiro MIKURIYA,^{†,††} Shigeo KIDA,[†] and Yoshie KONISHI

Department of Chemistry, Ibaraki University, Bunkyo, Mito 310

[†]Institute for Molecular Science, Myodaiji, Okazaki 444

(Received March 7, 1988)

Ternary cobalt(III) complexes with a general formula β_2 -[Co(tfac₂en)(L-aa)], where tfac₂en is the titled Schiff base ligand and L-aa denotes L-ala, L-leu, L-phe, L-tyr, and L-trp, were synthesized and separated into two diastereoisomers. On the bases of X-ray crystal analysis of the L-phe complex, CD, and ¹H and ¹⁹F NMR spectra, the structure of (–)₄₃₅- and (+)₄₃₅-isomers was determined to be *A*- and *A*-cis- β_2 -forms, respectively, and preferred conformation of the coordinated L-amino acidates was assumed to be *h*-form in solution. All the complexes showed stereoselectivity for the *A*-isomer in acetone and methanol, but the selectivity decreased or reversed with addition of water. The solvent-dependent stereoselectivity was explained in terms of steric repulsion and hydrophobic interligand interactions between CF₃ group of tfac₂en and side chain of L-aa.

Of various interligand interactions in metal complexes, hydrophobic intramolecular ligand-ligand interactions had been regarded as extremely weak. However, it has recently been proved that this kind of interaction plays an important role in molecular recognition and/or chiral recognition in some metal chelates.^{1–7)} For instances, Sigel and his co-workers,³⁾ and Yamauchi and his co-workers⁴⁾ found that the ternary metal(II) complexes with diamines such as 1,10-phenanthroline and amino acidates show a high ligand selectivity due to intramolecular hydrophobic interligand interaction between the diamine chelate ring and the side chain of amino acidates. Okawa et al.⁶⁾ demonstrated that metal(III) chelates with *l*-menthol derivatives exhibit a high stereoselectivity for *A*-configuration on the basis of intramolecular interligand CH– π interactions.

In order to elucidate the effect of hydrophobic interligand interactions on the stereoselectivity of metal complexes with chiral amino acidates, we prepared the cobalt(III) complexes described in the title containing Schiff base ligand with hydrophobic CF₃ groups (tfac₂en) and L-amino acidates (L-aa) with hydrophobic side chains as shown in Fig. 4, and investigated their steric structure and solvent dependency of stereoselectivity.

Experimental

Preparation of Complexes. Complexes were prepared from [Co(tfac₂en)] (0.01 mol) and amino acids (0.011 mol) by air oxidation in methanol–water by means of a similar method to that for β_2 -[Co(tfac₂en)(L-met)].⁸⁾ The crude reaction products were purified and/or separated into pure dia-

stereoisomers by the following methods. The data of elemental analysis and the optical rotation of all the complexes are summarized in Tables 1 and 2, respectively.

1) β_2 -[Co(tfac₂en)(L-phe)], β_2 -[Co(tfac₂en)(L-leu)], and β_2 -[Co(tfac₂en)(L-met)]. The crude reaction product (3.0 g) was dissolved in methanol (100 cm³) and filtered. The filtrate was slowly concentrated to a small volume at room temperature in 3–5 days to give massive dark green crystals ((–)₄₃₅-isomer, about 2.5 g). A single crystal of L-phe complex, thus obtained, was used for X-ray diffraction study.

The (–)₄₃₅-isomer (2.0 g) was dissolved in hot methanol (100 cm³) and water (10 cm³) was added to it. The solution was slowly concentrated to almost dryness at room temperature to give a large amount of massive crystals ((–)₄₃₅-isomer) and a small amount of needle-shaped crystals ((+)₄₃₅-isomer). The needle-shaped crystals were sorted by hand. Yield of (+)₄₃₅-isomer; 0.05–0.1 g for L-phe and L-met complexes, 0.3–0.5 g for L-leu complex.

2) β_2 -[Co(tfac₂en)(L-tyr)]. The crude reaction product was recrystallized from methanol to give light green needle-shaped crystals ((+)₄₃₅-isomer) in about 90% yield.

The recrystallization of the (+)₄₃₅-isomer from methanol–water (15:1 in volume) produced a large amount of (+)₄₃₅-isomer and a small amount of massive crystals ((–)₄₃₅-isomer, 0.05 g).

3) β_2 -[Co(tfac₂en)(L-ala)] and β_2 -[Co(tfac₂en)(L-trp)]. Recrystallization of the crude reaction product from methanol gave a 1:1 mixture of (–)₄₃₅- and (+)₄₃₅-isomers in about 90% yield. Acetone solution of the 1:1 mixture (0.2 g) was charged on a silica-gel column (Wakogel C-200, 15(φ)×120 mm), and was eluted with acetone at a flow rate of ca. 0.1 cm³ s^{–1}. The first green fraction (40 cm³) was collected and concentrated to dryness. In the case of L-trp complex, pure (–)₄₃₅-isomer was obtained by this procedure, but in the case of L-ala complex, a 4:1 mixture of (–)₄₃₅- and (+)₄₃₅-isomers of 70 mg was obtained.

Crystal Structure Determination. A Rigaku AFC-5 automated four-circle diffractometer was used at 25±1 °C. Crystal data and details of the data collection are given in Table 4. Lattice constants were determined by the least-squares refinement based on 40 reflections with 20 < 2θ < 30°.

^{††} Present address: Department of Chemistry, Faculty of Science, Kwansei Gakuin University, Uegahara, Nishinomiya 662.

The intensity data were corrected for Lorentz-polarization effects and for absorption. The structure was solved by the direct method. Refinements were carried out by the block-diagonal least-squares method. The absolute configuration was determined on the basis of the known configuration of L-phenylalanine. The absolute structure was further checked by performing cycles on two possible configurations, of which lower *R* factor was considered as the correct one. Hydrogen atoms were inserted in their calculated positions and fixed at their positions with B of 7 Å². The final discrepancy factors are *R*(F) 0.054 and *R*_w(F) 0.059 for 2294 unique reflections.

The atomic scattering factors and anomalous dispersion corrections were taken from Ref. 9. All the calculations were carried out on HITACHI M-680H computer at the Computer Center of the Institute for Molecular Science using a local version of MULTAN 78,¹⁰ UNIX-III,¹¹ and ORTEP¹² programs. Atomic coordinates are listed in Table 5. The anisotropic thermal parameters of non-hydrogen atoms, the atomic coordinates and thermal parameters of hydrogen atoms, and the *F*_o–*F*_c tables have been deposited as a Document No. 8827 at the office of Editor.

Measurements. The ¹H and ¹⁹F NMR spectra were measured with Hitachi R-20 (60MHz), JEOL GSX-400

(400MHz), and Varian CFT-20 (80MHz) spectrometers at an ambient probe temperature using TMS or fluorobenzene as internal references. The electronic absorption spectra and CD spectra were recorded with JASCO UBIDEC-1 spectrometer and JASCO J-20 spectropolarimeter, respectively, at room temperature. The optical rotations at 435 nm were measured with a JASCO DIP-140 polarimeter with 1 cm cell by the use of a thermostated cell-holder (the deviation of the solution temperature = ±0.1 °C). When the mutarotation was slow, the solutions were placed in a thermostated bath, and picked up one by one at proper intervals. The observed isomerization rate constant was calculated from the slope of plots for ln(α_∞–α_t) vs. time, where α_∞ and α_t denote the optical rotations under the equilibrium conditions and time *t*, respectively. The isomeric ratio, *K*=[(–)₄₃₅-isomer]/[(+)₄₃₅-isomer], under the equilibrium conditions was calculated from the equation, *K*=[*M*]_Δ^T–[*M*]_∞^T/([*M*]_∞^T–[*M*]_Δ^T), where [*M*]_Δ^T, [*M*]_∞^T, and [*M*]_∞^T represent the molar rotations at a temperature *T* of (+)₄₃₅-isomer, (–)₄₃₅-isomer, and under equilibrium conditions, respectively. In the cases of L-ala and L-trp complexes, the *K* values were estimated by assuming [*M*]_Δ^T=[*M*]_∞^T. The isomeric composition of all the isolated diastereoisomers was determined on the basis of their ¹H NMR spectra in CD₃OD.

Table 1. Elemental Analyses Data and Isomeric Composition of Complexes

Number of complex	Composition of isomer	Formula	Found(Calcd)		
			C(%)	H(%)	N(%)
1	a)	[Co(tfac ₂ en)(L-ala)]	38.03(37.75)	3.60(3.80)	8.92(8.81)
2	b)	[Co(tfac ₂ en)(L-ala)]	38.42(37.75)	3.91(3.80)	8.85(8.81)
3	(–) ₄₃₅ -ΔL-β ₂	[Co(tfac ₂ en)(L-leu)]	41.69(41.63)	4.38(4.66)	8.01(8.06)
4	(+) ₄₃₅ -ΔL-β ₂	[Co(tfac ₂ en)(L-leu)]	41.74(41.63)	4.41(4.66)	7.86(8.06)
5	(–) ₄₃₅ -ΔL-β ₂	[Co(tfac ₂ en)(L-met)]	38.01(38.00)	3.90(4.13)	7.91(7.82)
6	(+) ₄₃₅ -ΔL-β ₂	[Co(tfac ₂ en)(L-met)]	38.09(38.00)	4.05(4.13)	7.86(7.82)
7	(–) ₄₃₅ -ΔL-β ₂	[Co(tfac ₂ en)(L-phe)]	45.55(45.58)	3.87(4.01)	7.61(7.59)
8	(+) ₄₃₅ -ΔL-β ₂	[Co(tfac ₂ en)(L-phe)]	45.65(45.58)	3.85(4.01)	7.49(7.59)
9	(–) ₄₃₅ -ΔL-β ₂	[Co(tfac ₂ en)(L-tyr)] · H ₂ O	42.78(42.94)	4.10(4.12)	7.22(7.15)
10	(+) ₄₃₅ -ΔL-β ₂	[Co(tfac ₂ en)(L-tyr)]	44.46(44.30)	3.65(3.89)	7.51(7.38)
11	(–) ₄₃₅ -ΔL-β ₂	[Co(tfac ₂ en)(L-trp)]	46.03(45.41)	3.91(3.81)	7.15(7.21)
12	a)	[Co(tfac ₂ en)(L-trp)]	45.37(45.41)	3.70(3.81)	9.33(9.21)

a) 1:1 mixture of (–)₄₃₅-ΔL- and (+)₄₃₅-ΔL-β₂-isomers. b) 4:1 mixture of (–)₄₃₅- and (+)₄₃₅-isomers.

Table 2. Molar Rotation and Stereoselectivity of β₂-[Co(tfac₂en)(L-aa)] in Methanol

L-aa	Number of complex	[<i>M</i>] ₄₃₅ ²⁵ soon after dissolution	[<i>M</i>] ₄₃₅ ²⁵ equilibrium condition	Observed isomerization rate constant <i>k</i> _{obsd} /10 ^{–5} s ^{–1}	Isomeric ratio [<i>A</i>]/[<i>A</i>]
L-ala	1	–100 ^{a)}	–5200	13.4	1.2
	2	–29600 ^{b)}			
L-leu	3	–51200	–650	6.97	1.01
	4	+50500			
L-met	5	–47000	–3500	9.52	1.15
	6	+46800			
L-phe	7	–56300	–10500	7.45	1.41
	8	+54200			
L-tyr	9	–55000	–20200	5.50	2.14
	10	+54300			
L-trp	11	–54000	–28400	8.95	3.2
	12	0 ^{a)}			

a) 1:1 mixture. b) 4:1 mixture.

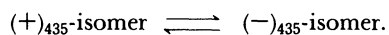
Table 3. ¹H and ¹⁹F NMR Spectral Data of β₂-[Co(tfac₂en)(L-aa)]^{a)}

L-aa	Number of complex and isomer form		tfac ₂ en				R-group of L-aa
			CH=C	CH ₂ CH ₂	CH ₃	CF ₃	
L-ala	2^{c)}	<i>A</i>	5.74	3.86	2.46	-11.93	1.37
			5.79			-12.31	1.49
	1^{b)}	<i>ΔΔ^{e)}</i>	5.72	3.86	2.46	-11.97	1.49
L-leu	3	<i>A</i>	5.84			-12.41	1.61
			5.74	3.84	2.46	-11.95	0.95
	4	<i>Δ</i>	5.80			-12.22	1.05
L-met	5	<i>A</i>	5.74	3.85	2.46	-11.99	0.95
			5.84			-12.54	1.05
	6	<i>Δ</i>	5.70	3.84	2.48	-11.78	2.14
L-phe	7	<i>A</i>	5.74			-12.13	
			5.70	3.84	2.48	-11.92	2.14
	8	<i>Δ</i>	5.78			-12.49	
L-tyr	9	<i>A</i>	5.58	3.60	2.11	-11.93	7.32
			5.71		2.43	-12.46	
	10	<i>Δ</i>	5.71	3.85	2.41	-11.88	7.38
L-trp	11	<i>A</i>	5.76		2.49	-13.01	
			5.56	3.61	2.18	d)	6.7—7.4
	12^{b)}	<i>ΔΔ^{e)}</i>	5.68		2.48		
			5.70	3.85	2.46	d)	6.7—7.4
			5.75		2.54		
			5.05	3.84	1.71	-11.97	7.0—7.7
			5.62		2.39	-12.59	
			5.60	3.84	2.39	-11.85	7.0—7.7
			5.73		2.49	-12.94	

a) ¹H: Soon after dissolution in CD₃OD; ¹⁹F: in CD₃COCD₃ (Ref.=Fluorobenzene). b) 1:1 mixture of *A*- and *Δ*-isomers. c) 4:1 mixture of *A*- and *Δ*-isomers. d) Scarcely soluble in CD₃COCD₃. e) NMR data for *Δ*-isomer is cited.

Results and Discussion

Properties of Complexes. All the complexes exhibited a mutarotation in methanol to show a minus rotation under equilibrium conditions (Table 2). For each amino acidato complex, the rotation in the equilibrium conditions of (−)₄₃₅-isomer was the same as that of (+)₄₃₅-isomer, and the plots of ln(α_∞−α_t) vs. time gave a linear relation in which the slope for (−)₄₃₅-isomer was identical as that for (+)₄₃₅-isomer. Hence, the observed mutarotation corresponds to the isomerization between two species of isomer, and the following equilibrium is established for each complex in methanol:¹³⁾



The isomerization occurred readily in methanol, ethanol, 1-propanol, and a mixed solvent of acetone and water, but was very slow in pure acetone, chloroform, *N,N*-dimethylformamide, and dimethyl sulfoxide.

The ¹H NMR spectra (Table 3) of complexes **3—11** soon after dissolution in methanol correspond to the spectra of only one species of isomer, indicating that the complexes **3—11** were isolated as pure isomer. On the other hand, the ¹H NMR of complexes **1** and **12** soon after dissolution correspond to the spectra of a 1:1 mixture of two isomeric species, and the ¹H NMR of complex **2** to that of a 4:1 mixture. The isomeric

compositions for all the complexes are listed in Table 1.

As the complexes are labile for isomerization in methanol, the ¹H NMR of all the complexes exhibited a time dependence in CD₃OD. The ¹H NMR under the equilibrium conditions corresponded to those for a mixture of two species of isomer, and the isomeric ratio of each amino acidato complex coincided with that determined from the optical rotation (Table 2). The isomeric ratios in Table 2 indicate that all the complexes show a stereoselectivity for *Δ*-isomer in methanol and the selectivity increases in the order of L-leu < L-met < L-ala < L-phe < L-tyr < L-trp. This order is almost parallel with the increasing order of steric bulkiness of the side chain of L-amino acidates, hence the steric repulsion between the side chain and Schiff base ligand seems to be responsible mainly to the stereoselectivity, as has been seen in β₂-[Co(α-Me-sal₂en)(L-aa)].¹⁴⁻¹⁷⁾ However, the stereoselectivity of β₂-[Co(tfac₂en)(L-aa)] is much lower than that of β₂-[Co(α-Me-sal₂en)(L-aa)]. This lower selectivity is due to the presence of CF₃ groups on the tfac₂en skeleton, and will be discussed later in detail.

The complexes readily isomerize in methanol, and when they are recrystallized from methanol, only one diastereoisomer or the 1:1 mixture of two isomers crystallized preferentially, as mentioned in Experimental section. Since the solubility of the preferentially crystallizing isomer in methanol was clearly

lower than that of the other isomer, the observed preferential crystallization corresponds to the second-order asymmetric transformation. Thus, in order to isolate more soluble isomer, we used a mixed solvent of methanol and water to lower the solubility. L-Ala and L-trp complexes were subjected to silica-gel column chromatography by use of acetone as an eluent to separate two isomers. However, silica-gel promoted isomerization of the complexes in acetone, so that only the $(-)$ ₄₃₅-isomer was separated.

Structure of Complexes. The results of X-ray structural analysis for $(-)$ ₄₃₅-[Co(tfac₂en)(L-phe)] are shown in Fig. 1 and numerical data are summarized in Tables 4, 5, and 6. The tfac₂en ligand takes *cis*- β - configuration and L-phenylalaninate coordinates as a bidentate ligand in forming a meridional N₃O₃ structure (*cis*- β ₂ structure). The absolute configuration was determined to be *A* on the basis of the known absolute configuration, *S*(C), of the asymmetric carbon atom of L-phenylalaninate. The *A*- β ₂-structure has been observed also for the $(-)$ ₄₃₅-isomer of [Co(tfac₂en)(L-met)]⁸⁾ and [Co(α -Me-sal₂en)(L-ile)]¹⁵⁾. The bond lengths (Co-N and Co-O) and angles (N-Co-O,

N-Co-N, and O-Co-O) of $(-)$ ₄₃₅-[Co(tfac₂en)(L-phe)] are close to those of $(-)$ ₄₃₅-[Co(tfac₂en)(L-met)], indicating that the steric structures of both complexes are essentially the same. In fact, not only they take the *A*- β ₂-structure but also they take *t* conformation for coordinated amino acidates.^{17,18)} However, the bond length of Co-O(3), 1.891(4) Å, of L-phe complex is longer than that of L-met complex, 1.849(9) Å. Since the phenyl group of L-phe seems to approach to some extent to the π -conjugation system of β -diketone-iminate part of tfac₂en (the closest interatomic distances; C(17)⋯C(7)=3.617(9) Å, C(17)⋯C(11)=4.050(9) Å, C(16)⋯C(8)=4.624(9) Å, and C(18)⋯F(6)=5.030(10) Å), the elongation of Co-O(3) bond length in L-phe complex may come from weak stacking between phenyl group and π -conjugation system of tfac₂en, although the dihedral angle between them is 132.5°.

The data for electronic absorption and CD spectra of the complexes are summarized in Table 7, and the representative spectra are shown in Fig. 2, together with the vicinal CD curves. Since the AB and CD spectra of $(-)$ ₄₃₅-isomers are very similar to those of $(-)$ ₄₃₅-*A*- β ₂-isomer of L-phe complex whose structure

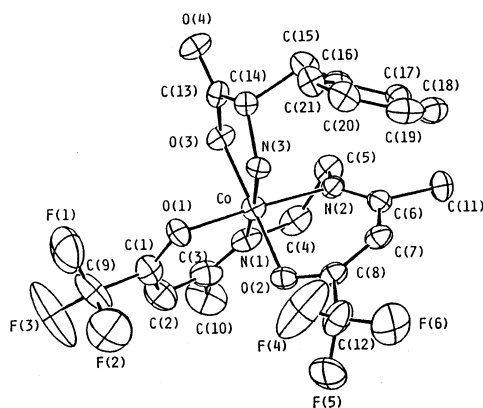


Fig. 1. A perspective drawing of $(-)$ ₄₃₅-*A*- β ₂-[Co(tfac₂en)(L-phe)] with the numbering of atoms.

Table 4. Crystal Data and Data Collection Details

Compound CoC₂₁H₂₂N₃O₄F₆, Formula Weight 553.35, Crystal system orthorhombic, Space group *P*2₁2₁2₁, *a*/Å 12.628(1), *b*/Å 21.490(2), *c*/Å 8.959(1) *V*/Å³ 2431.3(4), *Z* 4, *D_c*/g cm⁻³ 1.51, *D_m*/g cm⁻³ 1.52 *F*(000) 1128, Radiation graphite-monochromated Mo *K*α (*λ*=0.71073 Å), Crystal size/mm 0.33×0.33×0.57, *μ*(Mo *K*α)/cm⁻¹ 7.78, Scan type θ -2 θ , Scan Speed/deg min⁻¹ 3, Scan width/deg 1.1+0.5 tan θ , 2 θ Range/deg 1.5–64, Total No. of obsd reflcns 4740, No. of unique reflcns with $|F_o| > 3\sigma(|F_o|)$ 2294, Final No. of variables 317, Final residuals^{a)} *R*=0.054, *R_w*=0.059, Weighting scheme $w=[\sigma^2_{\text{count}} + (0.015|F_o|)^2]^{-1}$, Goodness of fit^{b)} 2.011, Largest peak on final difference Map 0.58 e Å⁻³

a) $R = \sum ||F_o| - |F_c|| / \sum |F_o|$; $R_w = [\sum W(|F_o| - |F_c|)^2 / \sum W|F_o|^2]^{1/2}$. b) $\text{GOF} = [\sum W(|F_o| - |F_c|)^2 / (N_{\text{observns}} - N_{\text{params}})]^{1/2}$.

Table 5. Atomic Coordinates ($\times 10^4$) and Thermal Parameters

Atom	X	Y	Z	<i>B</i> _{eq} /Å ²
Co	4353(1)	596(1)	4299(1)	3.6
F1	4898(6)	-1222(3)	6741(7)	12.8
F2	6263(6)	-738(3)	7197(7)	15.6
F3	6194(8)	-1473(3)	5592(8)	18.3
F4	5671(7)	1401(3)	8305(5)	16.6
F5	6992(4)	1564(2)	6998(8)	11.6
F6	6004(5)	2284(2)	7517(6)	10.7
O1	4700(3)	-130(2)	5353(5)	4.8
O2	5495(3)	995(2)	5346(4)	4.3
O3	3178(3)	185(2)	3437(4)	4.0
O4	1486(3)	-52(2)	3767(4)	5.0
N1	5174(4)	382(2)	2553(6)	4.6
N2	4075(4)	1367(2)	3261(5)	4.0
N3	3392(4)	764(2)	5967(5)	3.3
C1	5457(6)	-478(3)	4938(8)	5.4
C2	6033(6)	-459(3)	3638(9)	6.8
C3	5817(6)	-60(3)	2424(8)	5.5
C4	4955(6)	818(4)	1286(7)	5.9
C5	3971(6)	1204(3)	1636(7)	5.1
C6	4258(5)	1905(3)	3729(7)	4.4
C7	4731(5)	1989(3)	5184(7)	4.4
C8	5344(5)	1566(3)	5775(7)	4.4
C9	5732(8)	-990(4)	6099(9)	8.8
C10	6425(7)	-165(4)	999(10)	8.5
C11	4075(6)	2480(3)	2780(10)	6.5
C12	5962(8)	1694(3)	7168(9)	7.2
C13	2277(5)	205(2)	4158(6)	3.7
C14	2278(4)	607(3)	5558(6)	3.5
C15	1634(5)	1234(3)	5260(7)	4.7
C16	1726(5)	1677(3)	6527(7)	3.8
C17	2004(5)	2277(3)	6211(7)	5.0
C18	2092(6)	2724(3)	7368(10)	6.2
C19	1940(6)	2545(4)	8806(8)	6.9
C20	1670(6)	1927(3)	9123(8)	5.8
C21	1544(6)	1498(3)	7999(8)	5.0

Table 6. Interatomic Distances (Å) and Bond Angles (deg)

(a) Cobalt coordination spheres				Angle			
Distance							
Co-O(1)	1.876(4)	Co-N(1)	1.932(5)	Co-O(1)-C(1)	121.2(4)	C(7)-C(6)-C(11)	117.8(6)
Co-O(2)	1.921(4)	Co-N(2)	1.933(5)	O(1)-C(1)-C(2)	129.1(7)	C(6)-C(7)-C(8)	121.5(6)
Co-O(3)	1.891(4)	Co-N(3)	1.959(4)	O(1)-C(1)-C(9)	112.9(6)	C(7)-C(8)-O(2)	128.7(6)
Angle				C(9)-C(1)-C(2)	118.1(7)	O(2)-C(8)-C(12)	110.1(5)
O(1)-Co-O(2)	87.2(2)	O(2)-Co-N(3)	90.6(2)	C(1)-C(2)-C(3)	124.7(7)	C(7)-C(8)-C(12)	121.2(6)
O(1)-Co-O(3)	90.0(2)	O(3)-Co-N(1)	88.8(2)	C(2)-C(3)-N(1)	121.0(7)	Co-O(2)-C(8)	117.1(4)
O(1)-Co-N(1)	94.9(2)	O(3)-Co-N(2)	93.5(2)	C(2)-C(3)-C(10)	117.6(7)	C(1)-C(9)-F(1)	112.7(8)
O(1)-Co-N(2)	176.5(2)	O(3)-Co-N(3)	84.9(2)	C(10)-C(3)-N(1)	121.4(7)	C(1)-C(9)-F(2)	108.9(7)
O(1)-Co-N(3)	85.1(2)	N(1)-Co-N(2)	84.9(2)	Co-N(1)-C(3)	126.9(5)	C(1)-C(9)-F(3)	116.1(7)
O(2)-Co-O(3)	174.9(2)	N(1)-Co-N(3)	173.7(2)	Co-N(1)-C(4)	111.5(4)	F(1)-C(9)-F(2)	104.0(7)
O(2)-Co-N(1)	95.7(2)	N(2)-Co-N(3)	95.5(2)	C(3)-N(1)-C(4)	121.6(6)	F(1)-C(9)-F(3)	102.6(8)
O(2)-Co-N(2)	89.4(2)			N(1)-C(4)-C(5)	109.6(5)	F(2)-C(9)-F(3)	111.8(9)
(b) tfac ₂ en moiety				C(4)-C(5)-N(2)	104.7(5)	C(8)-C(12)-F(4)	115.5(8)
Distance				Co-N(2)-C(5)	106.4(4)	C(8)-C(12)-F(5)	111.9(7)
O(1)-C(1)	1.269(8)	C(6)-C(11)	1.518(10)	Co-N(2)-C(6)	126.7(4)	C(8)-C(12)-F(6)	113.5(7)
C(1)-C(2)	1.374(11)	C(7)-C(8)	1.307(9)	C(5)-N(2)-C(6)	123.8(5)	F(4)-C(12)-F(5)	105.8(8)
C(1)-C(9)	1.555(11)	C(8)-O(2)	1.300(7)	N(2)-C(6)-C(7)	119.7(6)	F(4)-C(12)-F(6)	107.8(7)
C(2)-C(3)	1.411(11)	C(8)-C(12)	1.499(11)	N(2)-C(6)-C(11)	122.4(6)	F(5)-C(12)-F(6)	101.1(7)
C(3)-N(1)	1.255(9)	C(9)-F(1)	1.299(12)	(c) L-Phenylalaninate moiety			
C(3)-C(10)	1.507(12)	C(9)-F(2)	1.307(11)	Distance			
N(1)-C(4)	1.496(9)	C(9)-F(3)	1.274(12)	O(3)-C(13)	1.309(7)	C(16)-C(17)	1.366(9)
C(4)-C(5)	1.527(10)	C(12)-F(4)	1.253(10)	O(4)-C(13)	1.194(7)	C(17)-C(18)	1.418(11)
C(5)-N(2)	1.503(8)	C(12)-F(5)	1.339(11)	C(13)-C(14)	1.523(8)	C(18)-C(19)	1.358(12)
N(2)-C(6)	1.251(8)	C(12)-F(6)	1.307(9)	N(3)-C(14)	1.492(7)	C(19)-C(20)	1.402(11)
C(6)-C(7)	1.445(9)			C(14)-C(15)	1.597(9)	C(20)-C(21)	1.374(10)
				C(15)-C(16)	1.486(9)	C(21)-C(16)	1.393(9)
				Angle			
				Co-O(3)-C(13)	117.7(4)	C(14)-C(15)-C(16)	111.9(5)
				O(3)-C(13)-O(4)	124.6(5)	C(15)-C(16)-C(17)	117.8(6)
				O(3)-C(13)-C(14)	115.1(5)	C(15)-C(16)-C(21)	122.2(6)
				O(4)-C(13)-C(14)	120.3(5)	C(16)-C(17)-C(18)	120.6(6)
				Co-N(3)-C(14)	110.8(3)	C(17)-C(18)-C(19)	119.4(7)
				N(3)-C(14)-C(13)	109.3(4)	C(18)-C(19)-C(20)	119.7(7)
				N(3)-C(14)-C(15)	109.3(5)	C(19)-C(20)-C(21)	121.0(7)
				C(13)-C(14)-C(15)	109.9(4)	C(20)-C(21)-C(16)	119.4(6)

Table 7. AB and CD Spectral Data for β_2 -[Co(tfac₂en)(L-aa)]^{a)}

L-aa and No. of complex	AB (log ϵ)	CD ($\Delta\epsilon$)	L-aa and No. of complex	AB (log ϵ)	CD ($\Delta\epsilon$)
L-leu (3)	17.24(2.34)	17.54(+9.02)	L-tyr (9)	17.24(2.31)	17.54(+8.84)
	21.28(2.23, sh)	20.83(+4.96)		21.74(2.24, sh)	20.41(+5.12)
	24.39(2.78, sh)	25.00(-12.89)		24.79(2.72, sh)	25.00(-12.34)
	29.59(3.72)	30.86(-22.14)		29.59(3.71)	31.06(-20.70)
L-leu (4)	17.24(2.39)	17.54(-9.25)	L-tyr (10)	17.24(2.34)	17.54(-9.93)
	21.74(2.32, sh)	20.83(-6.11)		21.74(2.30, sh)	20.41(-5.57)
	24.39(2.80, sh)	25.00(+13.12)		24.39(2.76, sh)	25.00(+13.35)
	29.41(3.76)	30.70(+21.38)		29.76(3.71)	30.86(+22.24)
L-phe (7)	17.24(2.31)	17.54(+8.86)	L-trp (11)	17.24(2.30)	17.54(+9.95)
	21.74(2.24, sh)	20.41(+5.12)		21.28(2.25)	20.62(+5.76)
	24.39(2.73, sh)	25.00(-12.46)		24.39(2.77)	24.39(-12.94)
	29.41(3.70)	30.77(-20.37)		29.41(3.75)	30.30(-20.95)
L-phe (8)	17.24(2.34)	17.24(-8.94)	L-ala (2) ^{b)}	17.24(2.29)	17.54(+5.40)
	21.74(2.29, sh)	20.41(-5.06)		21.28(2.19)	18.18(+1.69)
	24.39(2.75, sh)	24.69(+12.36)		24.39(2.74)	24.21(+6.28)
	29.41(3.70)	30.86(+19.53)		29.41(3.70)	30.58(-11.61)

a) Solvent: DMF+CHCl₃(1 : 4 in volume). Wavenumbers are given in 10³ cm⁻¹. The data of L-met complexes have been published in Ref. 8. b) 4 : 1 mixture of *A*- and *A*- β_2 -isomers.

has been verified by X-ray analysis, the *A*- β_2 -structure can safely be assigned to all the (-)₄₃₅-isomers. The AB spectra of (+)₄₃₅-isomers are also nearly identical with those of (-)₄₃₅-isomers, and the CD spectra of (+)₄₃₅-

isomers are almost the mirror image of those of (-)₄₃₅-isomers. Accordingly, *A*- β_2 -structure can be assigned to the (+)₄₃₅-isomers. Since the vicinal CD's of coordinated L-amino acidates show similar patterns with (-),

(+), and (−), signs from lower to higher energy in the first absorption region (16–23 cm^{-1}), the coordinated amino acidates are assumed to take a very similar coordination structure to each other.

Generally, amino acids can take three conformations, *t*, *g*, and *h*, around the $\text{C}(\alpha)\text{--C}(\beta)$ bond.^{17,18)} In the cases of coordinated L-amino acidates in β_2 -[Co(Schiff base)(L-aa)], they take the *t* conformation exclusively in the solid state.^{8,15)} Thus, the *t* rotamer seems to be very stable in this system. However, this is not the case in solution. In solution, the Δ - β_2 -isomers of L-phe, L-tyr, and L-trp complexes show NMR spectra in which one of CH_3 and one of $\text{CH}=\text{C}$ signals for tfac₂en shift to a higher field due to the ring current effect of aromatic ring of amino acidates (Table 3). In the case of Δ - β_2 -isomers, one of CF_3 signals shifts to a higher field. These high-field shifts are expected only when the conformation of coordinated amino acidates

is *h* form, and in fact 400 MHz ^1H NMR spectral analysis of the L-phe complex indicates that the *h* conformer is predominant in acetone (Table 8). Therefore, we assume that all the complexes prepared here prefer the *h* conformation for the coordinated amino acidates in solution.

Stereoselectivity of Complexes. When the coordinated amino acidates take the *h* conformation, the side chain of amino acidates approaches to CH_3 group of chelate ring A (Fig. 3) in the case of Δ - β_2 -isomer. Whereas, in the case of Δ - β_2 -isomer, the side chain approaches to CF_3 group of chelate ring A'. Since the approach is closer in Δ - β_2 -isomer than in Δ - β_2 -isomer in the model consideration, the main reason why the complexes prefer the Δ -configuration rather than the Δ will be that the steric repulsion between the side chain of amino acidates and tfac₂en ligand is stronger in Δ -isomer than in Δ .

On the other hand, both the side chain of amino acidates and CF_3 group of tfac₂en ligand are hydrophobic. Thus, when we use a hydrophilic solvent, hydrophobic interaction, especially solvophobic interaction, may occur between side chain and CF_3 . In order to confirm the above assumption, the solvent effect on the stereoselectivity was investigated. The results are shown in Fig. 4. Here, we selected acetone

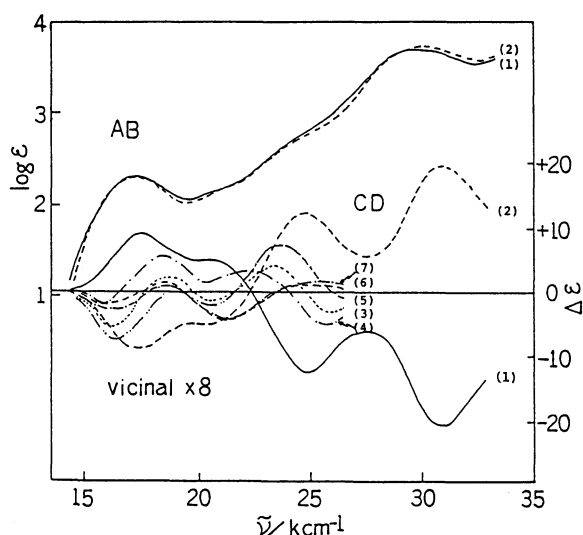


Fig. 2. Absorption (AB) and CD spectra of complexes in DMF- CHCl_3 (1:4) mixture. (1): $(-)^{435}\Delta$ - β_2 -[Co(tfac₂en)(L-phe)], (2): $(+)^{435}\Delta$ - β_2 -[Co(tfac₂en)(L-phe)], (3): vicinal CD of L-phe, (4), (5), (6), and (7) are vicinal CD's of L-trp, L-tyr, L-ala, and L-leu, respectively.

Table 8. Rotamer Populations about $\text{C}_\alpha\text{--C}_\beta$ Bond of Coordinated L-Phenylalaninate¹⁹⁾

Complex	J_{AC}	J_{BC}	Rotamer/%		
			<i>t</i>	<i>g</i>	<i>h</i>
Δ -L-Phe	4.8	5.6	29.4	22.0	48.6
Δ -L-phe	4.4	6.8	18.3	40.4	41.3

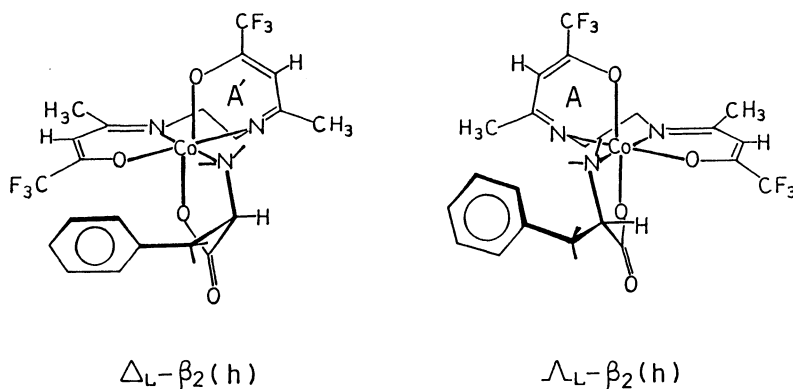
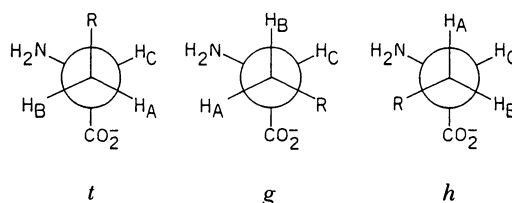


Fig. 3. Stereochemical relation between side chain of coordinated L-amino acidate (*h*-conformation) and tfac₂en ligand of Δ - and Δ - β_2 -isomers in solution.

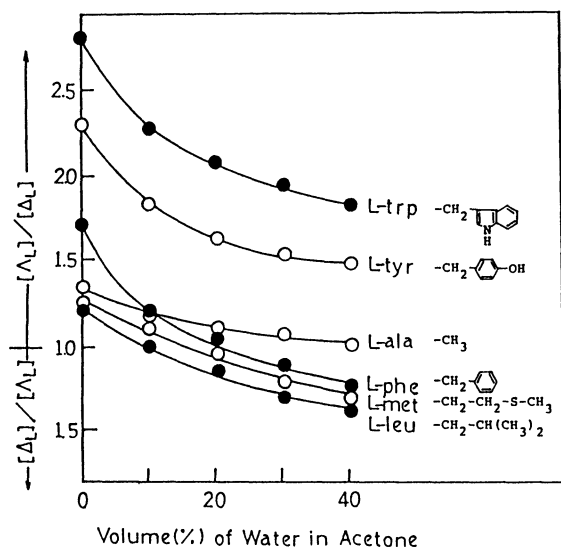


Fig. 4. Solvent dependence of stereoselectivity of β_2 - $[\text{Co}(\text{tfac}_2\text{en})(\text{L-aa})]$ at 25°C.

as a relatively hydrophobic solvent and investigated the effect of addition of water. Figure 4 indicates that 1) all the complexes prefer Δ -isomer in acetone, and the degree of the stereoselectivity is higher than that in methanol, and 2) the stereoselectivity decreases with addition of water and changes from Δ to Λ for L-leu, L-met, and L-phe complexes. The effect of addition of water is sensitive in the hydrophobic order of side chain of amino acidates, $\text{ala} < \text{met} < \text{leu} < \text{tyr} < \text{phe} < \text{trp}$, and the stereoselectivity for Δ -isomer increases in the hydrophilic order of solvents, $\text{acetone} < \text{methanol} < \text{water}$. Accordingly, hydrophobic interactions clearly contribute to the stereoselectivity of the employed complexes in water-acetone mixtures. The variation of the stereoselectivity with addition of water is the smallest for L-ala complex of all the complexes. This is due to the CH_3 group of L-alanine, which is too small to cause hydrophobic interaction with CF_3 group of tfac_2en . In comparison with L-ala, L-leu, and L-met complexes, the variation of stereoselectivity with addition of water is much larger in L-phe, L-tyr, and L-trp complexes. This fact indicates that the hydrophobic interactions with CF_3 group are stronger for aromatic side chains than for aliphatic ones. The stereoselectivity of L-tyr and L-trp complexes remains in favor of Δ -isomer even at 40% water content. This may be due to the fact that the side chain of L-tyr and L-trp have electronegative OH and NH groups, respectively, near aromatic rings, so that the electrostatic repulsion between CF_3 group and OH and NH groups reduces hydrophobic interactions.

From the above results and discussion, we conclude that 1) the complexes investigated here prefer Δ -isomer in acetone and methanol, and the selectivity is based mainly on the steric repulsion between the side chain of coordinated L-amino acidates and CF_3 group of

tfac_2en ligand in Δ -isomer, the counterpart of isomerization equilibrium, 2) in more hydrophilic solvents, the hydrophobic interactions occur between the above mentioned groups so as to increase the stereoselectivity for Δ -isomer, and 3) the hydrophobic interactions with CF_3 group is more effective when the side chain of amino acidates is aromatic group than aliphatic one.

References

- 1) H. Okawa and S. Kida, *Kagaku no Ryoiki*, **37**, 276 (1983).
- 2) R. M. Milburn, M. Gautam-Basak, R. Tribolet, and H. Sigel, *J. Am. Chem. Soc.*, **107**, 3315 (1985); R. Tribolet, R. Malini-Balakrishnan, and H. Sigel, *J. Chem. Soc., Dalton Trans.*, **1985**, 2291.
- 3) H. Sigel, R. Malini-Balakrishnan, and U. K. Häring, *J. Am. Chem. Soc.*, **107**, 5137 (1985); H. Sigel, R. Tribolet, and K. H. Scheller, *Inorg. Chim. Acta*, **100**, 151 (1985).
- 4) O. Yamauchi and A. Odani, *J. Am. Chem. Soc.*, **107**, 5938 (1985); A. Odani, S. Deguchi, and O. Yamauchi, *Inorg. Chem.*, **25**, 62 (1986).
- 5) Y. Numata, H. Okawa, and S. Kida, *Bull. Chem. Soc. Jpn.*, **53**, 2248 (1980).
- 6) M. Nakamura, H. Okawa, T. Inazu, and S. Kida, *Bull. Chem. Soc. Jpn.*, **55**, 2400 (1982); H. Okawa, K. Ueda, and S. Kida, *Inorg. Chem.*, **21**, 1594 (1982); M. Nakamura, H. Okawa, T. Ito, M. Kato, and S. Kida, *Bull. Chem. Soc. Jpn.*, **60**, 539 (1987).
- 7) K. Kashiwabara, I. Kinoshita, T. Ito, and J. Fujita, *Bull. Chem. Soc. Jpn.*, **54**, 725 (1981); M. Atoh, I. Kinoshita, K. Kashiwabara, and J. Fujita, *ibid.*, **55**, 3179 (1982).
- 8) K. Okamoto, K. Matsutani, and Y. Fujii, *Bull. Chem. Soc. Jpn.*, **58**, 3486 (1985).
- 9) "International Tables for X-Ray Crystallography," Kynoch Press, Birmingham (1974), Vol. 4.
- 10) P. Mani, S. E. Hull, L. Lessinger, G. Germain, J. P. Declercq, and M. M. Woolfson, MULTAN 78, A System of Computer Programs for the Automatic Solution of Crystal Structures from X-Ray Diffraction Data, University of York (1978).
- 11) T. Sakurai and K. Kobayashi, *Rikagaku Kenkyusho Hokoku*, **55**, 69 (1979).
- 12) C. K. Johnson, Report No. ORNL 3794, Oak Ridge National Laboratory, Oak Ridge, Tennessee (1965).
- 13) Y. Fujii, T. Kobayashi, M. Matsufuru, and S. Takahashi, *Bull. Chem. Soc. Jpn.*, **56**, 3608 (1983).
- 14) Y. Fujii, T. Isago, M. Sano, N. Yanagibashi, S. Hirasawa, and S. Takahashi, *Bull. Chem. Soc. Jpn.*, **49**, 3509 (1976).
- 15) Y. Kushi, R. Tamura, M. Kuramoto, T. Yoshizawa, H. Yoneda, and Y. Fujii, *J. Chem. Soc., Chem. Commun.*, **1978**, 266.
- 16) Y. Kushi, T. Tada, Y. Fujii, and H. Yoneda, *Bull. Chem. Soc. Jpn.*, **55**, 1834 (1982).
- 17) P. I. Vestues and R. B. Martin, *J. Am. Chem. Soc.*, **102**, 7906 (1980).
- 18) R. O. Gould, A. M. Gray, P. Taylor, and M. D. Walkinshaw, *J. Am. Chem. Soc.*, **107**, 5921 (1985).
- 19) The population was calculated from the coupling constants of ABX pattern for $-\text{CH}_2-\text{CH}-$ group of L-phe complex in acetone- d_6 by the use of method in Ref. 17.